Crystal Structures and Stereodynamics of Neutral Hexacoordinate Silicon Chelates: Use of an Optically Active Ligand for Assignment of an Intramolecular Ligand Exchange Process

Daniel Kost,*,† Inna Kalikhman,*,† Sonia Krivonos,† Dietmar Stalke,‡ and Thomas Kottke‡

Contribution from the Department of Chemistry, Ben Gurion University of the Negev, Beer-Sheva 84105, Israel, and Institut für Anorganische Chemie der Universität Würzburg, D-97074 Würzburg, Germany

Received August 26, 1997

Abstract: Crystal structures determined for several neutral hexacoordinate bis(N→Si) chelates revealed in all cases near octahedral geometries with the nitrogen ligands in relative trans and the monodentate ligands in cis positions. To assign the two consecutive intramolecular ligand-site exchange processes (reported earlier), a bis-chelate was prepared containing a chiral carbon center in each of the chelate rings (**14**). By means of a phase sensitive NOESY NMR spectrum it was possible to conclude that the lower-barrier process involved exchange of diastereotopic groups only *within* each diastereomer, and not between them, resulting in the assignment of this process to the direct nondissociative interchange of the monodentate ligands (X, Y). The Si−Cl bond lengths were found to inversely correlate with the lower of the activation barriers. Dissociation−recombination of the N→Si dative bond was also observed by the high-temperature NMR spectra. Lack of correlation between Si−N distances in the crystals and activation barriers led to the conclusion that Si−N dissociation was not involved in the measured rate processes, but followed, at slightly higher temperature, the epimerization at the silicon center by exchange of the two oxygen sites.

The structure and chemistry of hexacoordinate silicon chelates have been the focus of a number of recent studies.[1−5] However, only a few structural and stereodynamic studies have been reported, and they have been described as being still in an "embryonic stage".[3] Within the few known crystal structures of neutral bis(N→Si) chelates, the structural diversity is rather large: most of the reported crystal structures feature a "bicapped tetrahedral" geometry (**1**−**4**, Figure 1), in which the basic tetrahedral structure around silicon is retained, with two donor nitrogens coordinated opposite two faces of the tetrahedron.[6−9] By contrast, crystal structures of nearly octahedral bis(N→Si) complexes have also been reported recently (**5**,[10] **6**,[11] **7**,[11] **8**,[11] **9**[12]). The factors responsible for the solid-state structures of these complexes are not yet understood. In the present paper we report two new crystal structures of neutral dinitrogen-chelated silicon complexes, **10**, **11**, and discuss their geometries.

Hexacoordinate silicon complexes undergo a variety of inter-[13] and intramolecular[14] ligand-site exchange reactions, observable by NMR spectroscopy. In a previous publication we analyzed the stereodynamic behavior of a series of hexacoordinate bis(N→Si) complexes **8**−**11** and, on the basis of their multinuclear NMR spectra, concluded that they underwent two consecutive intramolecular ligand-site exchange reactions on the NMR time scale.[15−17] These two proposed processes were assigned to the interchange of adjacent ligands ("1,2-shift"), via a bicapped tetrahedron transition state or intermediate (Figure 2). One process involves the interchange of the two monodentate ligands (X,Y)-1,2-shift, while in the other process exchange of the two oxygens takes place. On the basis of the reported results it was not possible to individually assign each exchange process to one or the other observed barrier. Utilizing a chiral

† Ben Gurion University.

‡ Universität Würzburg.

(1) Tandura, St. N.; Alekseev, N. V.; Voronkov, M. G. *Top. Curr. Chem.* **1986**, *131*, 99.

(2) Corriu, R. J. P.; Young, J. C. In *The Chemistry of Organic Silicon Compounds;* Patai, S., Rappoport, Z., Eds.; Wiely: Chichester, U.K., 1989; p 1241.

(3) Holmes, R. R. *Chem. Rev.* **1996**, *96*, 927.

(4) Chuit, C.; Corriu, R. J. P.; Reye, C.; Young, J. C. *Chem. Rev.* **1993**, *93*, 1371.

(5) Kost, D.; Kalikhman, I. In *The Chemistry of Organic Silicon Compounds*; Apeloig, Y., Rappoport, Z., Eds.; Wiley: Chichester, U.K., in press.

(6) Breliere, C.; Carre, F.; Corriu, R. J. P.; Poirier, M.; Royo, G.; Zwecker, J. *Organometallics* **1989**, *8*, 1831.

(7) Carre, F.; Cerveau, G.; Chuit, C.; Corriu, R. J. P.; Reye, C. *New J. Chem.* **1992**, *16*, 63.

(8) Carre, F.; Chuit, C.; Corriu, R. J. P.; Mehdi, A.; Reye, C. *Organometallics* **1995**, *14*, 2754.

(9) Belzner, J.; Shar, D. In *Organosilicon Chemistry II;* Auner, N., Weis, J., Eds.; VCH: Weinheim, 1996; pp 459−465.

(10) Klebe, G.; Tran Qui, D. *Acta Crystallogr.* **1984**, *C40*, 476.

(11) Kalikhman, I.; Krivonos S.; Stalke, D.; Kottke, T.; Kost, D. *Organometallics* **1997**,*16*, 3255.

(12) Mozzhukhin, A. O.; Antipin, M. Yu.; Struchkov, Yu. T.; Gostevskii, B. A.; Kalikhman, I. D.; Pestunovich, V. A.; Voronkov, M. G. *Metalloorg. Khim.* **1992,** *5*, 658; *Chem. Abstr.* **1992**, *117*, 234095w.

(13) Farnham, W. B.; Whitney, J. F. *J. Am. Chem. Soc.* **1984**, *106*, 3992.

(14) (a) Breliere, C.; Corriu, R. J. P.; Royo, G.; Zwecker, J. *Organometallics* **1989,** *8*, 1834. (b) Breliere, C.; Carré, F.; Corriu, R. J. P.; Douglas, W. E.; Poirier, M.; Royo, G.; Wong Chi Man, M. *Organometallics* **1992**, *11*, 1586. (c) Carré, F.; Chuit, C.; Corriu, R. J. P.; Fanta, A.; Mehdi, A.; Reye, C. *Organometallics* **1995**, *14*, 194.

(15) Kalikhman, I.; Kost, D. *J. Chem. Soc., Chem. Commun.* **1995**, 1253.

(16) Kost, D.; Kalikhman, I.; Raban, M. *J. Am. Chem. Soc.* **1995**, *117*, 11512.

(17) Kost, D.; Krivonos, S.; Kalikhman, I. In *Organosilicon Chemistry III*; Auner, N., Weis, J., Eds.; VCH-Wiley: Weinheim, 1997; pp 435−445.

S0002-7863(97)03002-3 CCC: $15.00
Published on Web 04/18/1998

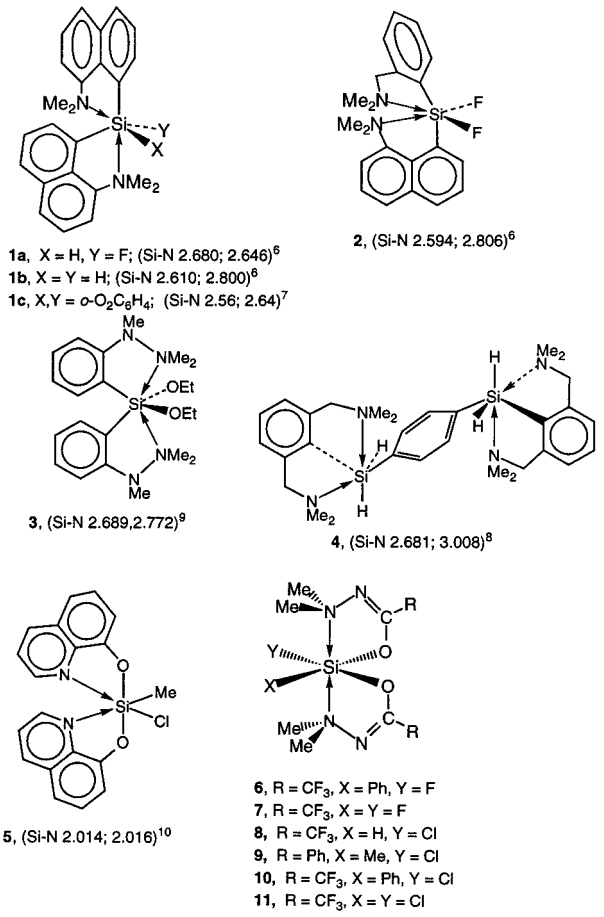

Figure 1. Hexacoordinate silicon chelates, and the corresponding Si−N bond lengths (Å). Literature references are shown where appropriate.

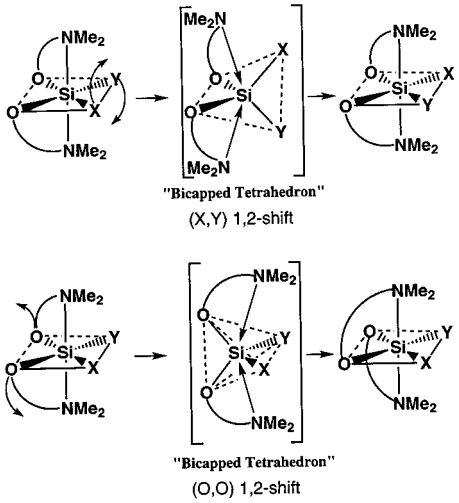

Figure 2. Ligand exchange mechanism by 1,2-shift of adjacent ligands, via a bicapped-tetrahedron intermediate or transition state: upper part, monodentate ligand (X−Y) interchange; lower part, oxygen−oxygen interchange.

carbon ligand, we have been able in the present study to discriminate between these two exchange reactions, and to definitely assign one of them.

Results and Discussion

(a) Crystallographic Structures. The preparation of complexes of the series **6**−**11** was described previously.[11,16] Figure 3 depicts the single-crystal X-ray structures for compounds **10** and **11**. These structures have the same near-octahedral

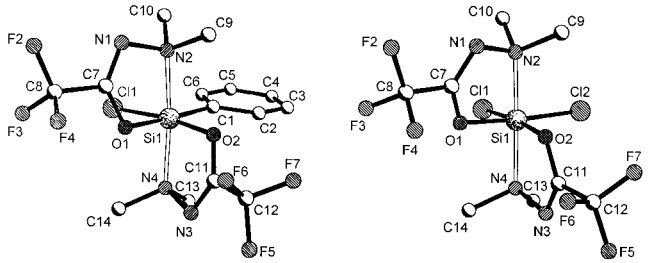

Figure 3. X-ray crystal structures for **10** (left) and **11** (right). Only one of the two unique molecules in the asymmetric unit of each crystal is shown. Hydrogen atoms have been omitted for clarity.

geometry reported previously for members of this series, and hence the octahedron is a characteristic geometry for this series, in contrast to **1**−**4** with the bicapped tetrahedral structure. The question now arises as to which complexes form octahedral and which tetrahedral molecular structures in the crystal. It appears that in **1**−**4**, the tetrahedral complexes, the number of electronegative ligands attached to silicon is smaller than in the octahedral complexes (**5**−**11**). A maximum of one Si−C bond is allowed in the octahedral complexes. When the number is greater than one, bicapped tetrahedral geometries are obtained in the solid state.

Tables 1 and 2 list various bond lengths and angles (respectively) extracted from the X-ray crystallographic determinations. Examination of the silicon−nitrogen distances confirms the previous observations that octahedral complexes are characterized by relatively short Si−N bond lengths (∼1.95−2.2 Å in intramolecular neutral chelates[3,4,12]), while in the bicapped tetrahedral structures the Si−N distances are greater than 2.5 Å.[3,4,6−9]

From Table 2 it is evident that the near-octahedral geometries are characterized by near 90° bond angles between the bonds connecting silicon to the various cis ligand pairs (O, N, X, Y). This is in contrast to the near 109° measured in bicapped tetrahedral complexes.[6−9]

Another question of interest relates to the relative orientation of the two nitrogen ligands: in all of the compounds of the series **6**−**11**, the nitrogens are trans relative to each other.[11,12] However, in **5**, in which the ligand environment around silicon is identical to that in **6**−**11**, the nitrogen ligands occupy cis positions.[10] Comparison with the analogous *inter*molecular adducts, $SiF_4 \cdot 2NH_3$ (**12**),[18] $SiF_4 \cdot$2pyridine (**13**),[19] shows that the latter adducts have the nitrogen ligands in trans positions, while the four fluoro ligands lie in an equatorial plane. It may be concluded that in the absence of steric constraints the nitrogen ligands prefer the trans geometry, and apparently in the single structure **5** in which they are cis to each other, the strained chelates force a cis geometry. This conclusion is also supported by the observation that the Si−N distances in **6**−**11** (Table 1) are very close to those found in the strain-free **12** and **13**, 1.895[18] and 1.935[19] Å, respectively.

(b) Stereodynamic Analysis. As mentioned earlier, two intramolecular ligand-site exchange reactions (shown in Figure 2) were proposed in a previous study for compounds of the type **6**−**11**.[15,16] These two exchange processes were each observed by coalescence of signals due to the diastereotopic *N*-methyl groups in the NMR spectra, and in most cases were well resolved and separated from each other on the temperature scale. In the lower of the two processes interconversion of the two chelate rings is observed, while in the second one complete

(18) Plitzko, C.; Meyer, G. Z. *Anorg. Allg. Chem.* **1996**, *622*, 1646.
(19) Bain, V. A.; Killean, R. C. G.; Webster, M. *Acta Crystallogr., Sect. B*, **1969**, *25*, 156.

Table 1. Selected Crystallographic Bond Lengths for Hexacoordinate Silicon Complexes (Å)

compd	R	X	Y	Si−N[a]	Si−N[b]	Si−O[b]	Si−O[a]	Si−Cl, Si−F	Si−C	ref
6	CF_3	Ph	F	2.029(3)	2.021(3)	1.817(2)	1.826(3)	1.638(2)	1.911(3)	11
7	CF_3	F	F	1.962(2)	1.962(2)	1.782(2)	1.782(2)	1.615(2)		11
8	CF_3	H	Cl	2.002(3)	2.002(3)	1.772(3)	1.772(3)	2.184(2)		11
9	Ph	Me	Cl	2.015(7)	2.036(6)	1.780(6)	1.771(6)	2.197(4)	2.089(8)	12
10[c]	CF_3	Ph	Cl	2.042(4)	2.046(4)	1.784(3)	1.808(3)	2.187(2)	1.908(4)	this work
				2.042(4)	2.045(4)	1.790(3)	1.804(3)	2.189(2)	1.921(4)	
11[c]	CF_3	Cl	Cl	2.011(2)	2.013(2)	1.775(1)	1.777(1)	2.141(1); 2.142(1)		this work
				2.010(2)	2.017(2)	1.774(1)	1.775(1)	2.147(1); 2.138(1)		

[a] Chelate trans to Ph. [b] Chelate trans to Cl, F. [c] For **10** and **11** geometric parameters for both molecules in the asymmetric unit are listed.

Table 2. Selected Bond Angles (deg) for Complexes **6**−**11**

compd	∠N−Si−N′	∠F(Cl)−Si−N	∠O−Si−N	∠O−Si−O	∠F(Cl)−Si−O
6	163.62(8)	91.23(12); 96.85(12)	85.29(10); 80.88(9) 82.42(10); 87.67(12)	85.16(9)	87.40(8); 170.58(7)
7	170.49(14)	91.12(9); 95.39(8)	89.24(8); 83.85(9)	86.95(9)	89.89(9); 174.09(9)
8	170.1(2)	95.20(10); 90.64(9)	83.42(11); 89.41(11)	87.7(2)	82.41(13)
9	170.7(3)	91.8(2)	81.5(3)	86.7(3)	86.3(2)
10[a]	164.7(2)	91.84(12); 93.09(12)	81.2(2); 84.6(2) 82.4(2); 90.6(2)	85.20(14)	86.31(11); 170.13(13)
	166.2(2)	90.38(12); 95.52(13)	83.0(2); 85.7(2) 82.4(2); 89.3(2)	85.08(14)	86.58(11); 169.71(13)
11[a]	168.73(7)	92.16(5); 94.09(5) 90.84(5); 98.28(5)	87.37(7); 83.22(7) 82.91(6); 90.60(7)	88.28(7)	89.53(5); 174.95(5) 90.40(6); 173.64(5)
	171.59(7)	91.33(5); 94.67(5) 91.75(5); 93.67(5)	83.09(6); 90.18(7) 83.33(6); 91.38(7)	88.13(7)	88.91(6); 173.64(15) 88.91(5); 174.26(5) 89.78(5); 173.99(5)

[a] For **10** and **11** geometric parameters for both molecules in the asymmetric unit are listed.

coalescence of *N*-methyl signals takes place. However, since *both* of the processes shown in Figure 2 involve interconversion of the chelate rings, assignment of each barrier to one or the other reaction was not possible. To reach such an assignment, complex **14**, in which two chiral centers have been incorporated in the chelate rings, was prepared from (*R*)-(−)-2-phenylpropionic acid according to the sequence shown in eq 1.

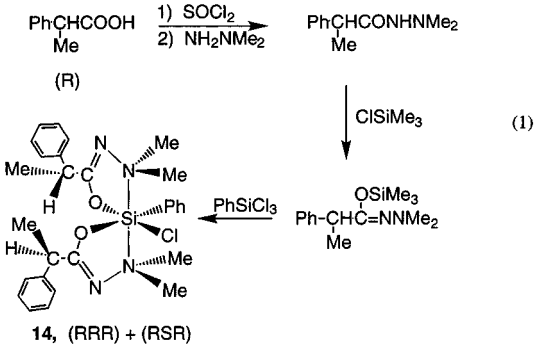

(1)

14 has a total of three chiral centers, one at silicon and two at carbons, and may exist in two diastereomeric forms: *R*−*R*−*R* and *R*−*S*−*R*, differing in the configuration at the silicon center. Indeed the low-temperature ^{1}H NMR spectrum (Figure 4) clearly shows two unequally populated isomers: the four *N*-methyl groups in each diastereomer give rise to four singlets (labeled 1 and 2, respectively), with relative signal intensities between the two groups of ca. 4:3. The same intensity distribution is found in the *C*-methyl signals (two doublets for each diastereomer) and the Me−C*H* signals (two quartets for each diastereomer). The coalescence phenomena of the latter signals were best resolved, and served for the evaluation of rate constants and activation free energies for the two exchange processes (in toluene-d_8, lower process for diastereomer **14-1**, $\Delta\nu = 165$ Hz, $T_{c1} = 335$ K, $\Delta G_1^* = 15.8 \pm 0.1$ kcal mol^{-1}; lower process for diastereomer **14-2**, $\Delta\nu = 11$ Hz, $T_{c1} = 300$ K, $\Delta G_1^* = 15.7 \pm 0.1$ kcal mol^{-1}; higher process, $\Delta\nu = 110$ Hz, $T_{c2} = 355$ K, $\Delta G_2^* = 17.0$ kcal mol^{-1}).[20]

We now examine the two rate processes, (Ph,Cl) and (O,O) exchange in **14**, in terms of their NMR-spectral consequences: the former effects interchange between the two chelate rings, such that the ring that was in a trans position relative to Cl becomes trans to the phenyl group, while that trans to phenyl is now opposite Cl. This process is a topomerization, by which diastereotopic groups exchange roles within the same diastereomer. It does not affect the chirality at any one of the chiral centers, and therefore does not exchange between diastereomers.

The (O,O) exchange, on the other hand, interchanges the two chelate rings and *in addition* inverts the configuration at the silicon center: *R*−*R*−*R* ⇄ *R*−*S*−*R*. Thus, this process involves exchange between the diastereomers and consequent coalescence of signals from one stereoisomer with those of the other.

It follows that if coalescence of signal pairs *within* each stereoisomer is observed during the lower energy exchange process, this process constitutes a (Ph,Cl) exchange. Conversely, if the lower of the two processes exchanges signals belonging to one of the diastereomers with those of the other, then (O,O) exchange is observed. The NMR consequences of the two possible alternative pathways are shown schematically in Figure 5.[21]

These expectations are borne out in the phase-sensitive 2D-NOESY experiment shown in Figure 6. The experiment was run in toluene-d_8 solution at 250 K, an intermediate temperature (below the coalescence temperatures) at which the higher of the two rate processes is too slow to be effective, while the

(20) We reported previously[16] on the substantial solvent dependence of the *N*-methyl exchange barriers in analogous complexes. This was also tested for **14**: the lower barrier measured in CD_2Cl_2, $T_{c1} = 223$ K, $\Delta\nu_1 = 200$ Hz, $\Delta G_1^* = 10.1$ kcal mol^{-1}; the higher process measured in nitrobenzene-d_5 solution, $T_{c2} = 350$ K, $\Delta\nu_2 = 77$ Hz, $\Delta G_2^* = 17.0$ kcal mol^{-1}.

(21) For a similar case, in which two consecutive rate processes were resolved by their different NMR consequences, see: Kost, D.; Egozy, H. *J. Org. Chem.* **1989**, *54*, 4909. Kost, D.; Zeichner, A.; Sprecher, M. S. *J. Chem. Soc., Perkin Trans. 2* **1980**, 317.

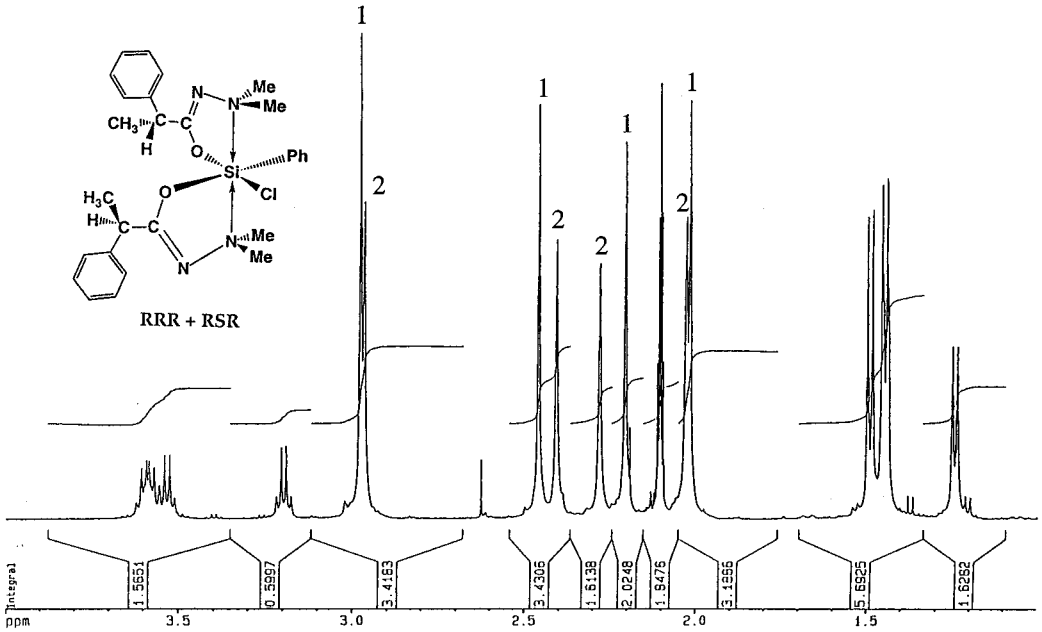

Figure 4. ^{1}H NMR spectrum of **14** at the slow exchange limit temperature, 250 K, in toluene-d_8 solution, featuring two diastereomers. Only the high-field portion is shown (the quintet at 2.1 ppm is due to the solvent).

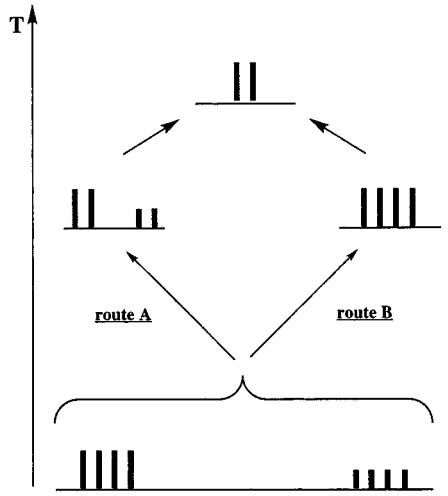

Figure 5. Two schematic routes for the ^{1}H NMR spectral changes associated with *N*-methyl exchange in **14** upon an increase of temperature: route A, exchange *within* each diastereomer; route B, exchange *between* diastereomers.

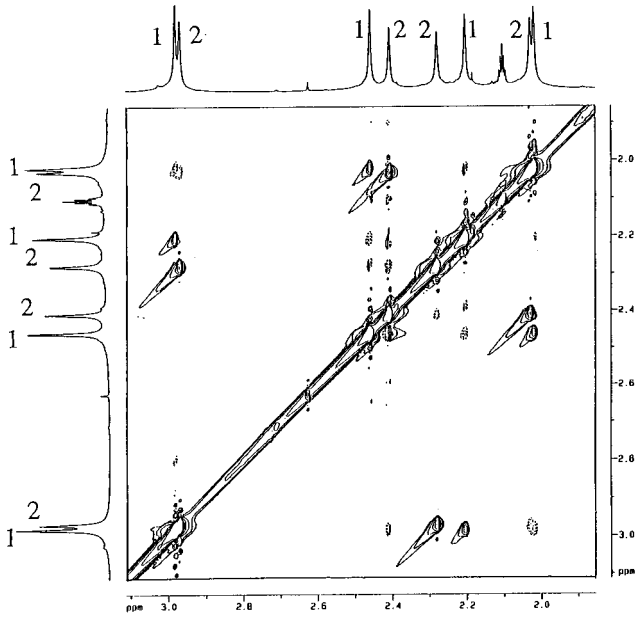

Figure 6. Phase-sensitive NOESY spectrum of **14** (*N*-methyl region) in toluene-d_8 at 250 K. Positive (exchange) cross-signals are drawn by solid lines, negative (NOE) cross-signals by dotted lines. Exchange (and NOE) cross-peaks connect *only* signals within the same diastereomer: 1 with 1 and 2 with 2.

faster process occurs at a significant rate. Negative (NOE) cross signals connect pairs of geminal *N*-methyl groups, which are near each other in space. The positive cross signals in Figure 6 connect pairs of interchanging signals. Clearly only signals belonging to the same diastereomer interchange in this rate process: signals of the high-intensity isomer (labeled 1) have positive cross-signals *only* with signals of the same isomer, and those labeled 2 exchange only with others labeled 2. It is thus concluded unequivocally that the rate process observed at lower temperature, with the lower activation barrier, represents 1,2-shift of the adjacent Ph,Cl ligands.

Support for the assignment of (Ph,Cl) exchange to the lower of the two exchange processes comes from an analysis of the X-ray crystallographic data. The activation barriers for this process for the chloro complexes (**8**−**10**) in toluene-d_8 solutions were reported (listed in order of increasing barrier):[16] **9** (X = Me), 13.7; **10** (X = Ph), 15.9; **8** (X = H), 17.5 kcal mol^{-1}. The order of increasing barriers for **8**−**10** corresponds roughly to the decrease in Si−Cl bond length in the crystal structures (Table 1). A reasonable inverse linear relationship is obtained ($\Delta G_1^* = -274 d_{Si-Cl} + 616$, $R = 0.977$). Such a correlation of bond lengths with activation energies generally suggests that dissociation of the bond is involved in the rate-determining part of the reaction sequence. However, earlier evidence (persistence of Si−F coupling constants in an analogous fluoro complex at elevated temperatures)[16] ruled out the possibility of intermolecular ligand exchange. The Si−Cl bond-length dependence of the barrier may also be consistent with a *nondissociative* (X,-Cl)-1,2-shift, assuming that the twist of the two ligands involves

elongation of the Si−ligand bonds, and hence that lower barriers should be expected in the case of longer ground-state Si−Cl bonds.

If indeed, as the data suggest, Si−Cl bond elongation accompanies the (X,Cl) exchange, then the distinction between a nondissociative vs an intramolecular-dissociative process becomes ill-defined: a Cl atom (or anion) may dissociate to a relatively large distance from silicon, followed by recombination, or it may *partially* dissociate (i.e., without complete cleavage of the bond at any point along the reaction coordinate), during the (X,Cl)-shift. The result in both cases is the same, and in fact, these two mechanisms represent the two ends of a mechanistic continuum. This mechanistic interpretation is in agreement with the observation of the Si−Cl bond length correlation with the barrier, as well as with the intense solvent dependence of the barriers.[16]

The second process, with the higher activation energy, is compatible with (O,O) exchange. However, at the fast exchange limit temperature for **14**, if only these two, (Ph,Cl) and (O,O), exchanges take place, the geminal *N*-methyl groups should remain diastereotopic and give rise to two singlets, as a result of the adjacent carbon chirality. In fact, a broad singlet is observed in toluene-d_8 solution up to 380 K. The geminal *N*-methyls can only become truly equivalent if Si−N dissociation, followed by fast rotation about the NN bond and recombination, become fast on the NMR time scale. This result leaves several open options: the observation that above coalescence the signal is slow to narrow, relative to other signals, suggests that either (a) a gradual change in the static chemical shifts with eventual accidental equivalence occurs, above the coalescence due to (O,O) exchange, or (b) a second rate process, Si−N cleavage, follows (O,O) exchange. A third possibility (c) might be a direct Si−N dative bond cleavage which brings about complete equivalence of the *N*-methyl groups, even without the (O,O) exchange mechanism.

Possibility (a) may be ruled out on the basis of a comparison with the methyl analogue of **14**, **15** (R = (±)-1-phenylethyl, X = Me, Y = Cl): at elevated temperature the ^{1}H NMR spectrum of **15** featured, like that of **14**, one singlet for the *N*-methyl groups. It is highly unlikely that accidental equivalence would be found in both compounds.

From Table 1 it is evident that the Si−N bond lengths do not correlate with the barrier for the second (slower) ligand exchange process (**8**, 18.0; **9**, 14.8; **10**, 16.3; **11**, 20.7 kcal mol^{-1}),[16] in the manner observed for the Si−Cl bonds and the first barrier. This suggests that Si−N dissociation is not involved in the rate-determining process measured by the spectral changes, but rather follows the (O,O) exchange at slightly higher temperature (option (b) above). Thus, the measured barrier is for the (O,O) exchange, while at the fast exchange limit temperature (after narrowing of the spectral lines) *both* processes ((O,O) exchange and N−Si dissociation) have already taken place, and hence a single resonance is observed for the *N*-methyl groups.

In conclusion, the presence of the chiral carbon centers leads to unequivocal NMR evidence that the first (faster) of the two observed rate processes in **14** and analogous complexes is exchange between adjacent monodentate ligands ((Ph,Cl)-1,2-shift). This is supported by comparison of Si−Cl crystallographic bond lengths and measured exchange barriers. At higher temperature, epimerization of the silicon center takes place via (O,O) exchange, followed by dissociation and recombination of the N−Si dative bond.

Table 3. Crystal Data of **10** and **11**

	10	**11**
formula	$C_{14}H_{17}ClF_6N_4O_2Si$	$C_8H_{12}Cl_2F_6N_4O_2Si$
fw	450.86	409.21
crystal size (mm^3)	0.4 × 0.3 × 0.3	0.5 × 0.5 × 0.4
space group	$P2_1/c$	$P\bar{1}$
a (Å)	9.135(2)	9.606(2)
b (Å)	26.969(3)	13.463(3)
c (Å)	15.818(4)	13.725(3)
α (deg)	90	110.112(12)
β (deg)	101.884(8)	104.037(13)
γ (deg)	90	96.07(2)
V (Å^3)	3813.4(11)	1581.7(6)
Z	8	4
temp (K)	173(2)	173(2)
ρ_{calc} (Mg m^{-3})	1.571	1.718
μ (mm^{-1})	0.338	0.561
F(000)	1840	824
2θ range (deg)	6−45	6−50
no. of reflections collected	5385	6334
no. of unique reflections (R_{int})	4901 (0.035)	5577 (0.009)
no. of restraints	198	10
no. of refined parameters	514	423
goodness of fit (all data)	1.048	1.033
$R1^a$ [$I > 2\sigma(I)$]	0.050	0.035
$wR2^b$ (all data)	0.116	0.072
g_1; $g_2{}^c$	0.0450; 1.8127	0.0325; 1.1252
largest diff peak/hole (e Å^{-3})	0.303/−0.288	0.446/−0.381

[a] $R1 = \sum||F_o| - |F_c||/\sum|F_o|$. [b] $wR2 = \{\sum[w(F_o^2 - F_c^2)^2]/\sum[w(F_o^2)^2]\}^{1/2}$. [c] $w = 1/[\sigma^2(F_o^2) + (g_1P)^2 + g_2P]$; $P = (F_o^2 + 2F_c^2)/3$.

Experimental Section

X-ray Measurements of 10 and 11. The crystal data for both structures are presented in Table 3. Crystals of **10** and **11** were mounted on the tip of a glass fiber, coated by a drop of perfluorinated polyether and shock-frozen in the cold nitrogen gas stream of the low-temperature device of the diffractometer.[22] Data were collected at −100 °C on an Enraf-Nonius CAD4 four-circle diffractometer, equipped with a homemade low-temperature device, using graphite-monochromated Mo Kα radiation (λ = 0.710 73 Å). The structures were solved by direct methods (SHELXS-90[23]) and refined to convergence by full-matrix, least-squares iteration against F^2 (SHELXL-96[24]) minimizing the function $w(F_o^2 - F_c^2)$ (Table 3). All non-hydrogen atoms were refined anisotropically. The hydrogen atoms were refined on calculated positions using a riding model. The isotropic displacement parameters of the hydrogen atoms were fixed to equal 1.2 times (aromatic CH) and 1.5 times (CH_3 group) the value of U_{eq} of the preceding carbon atom. A rotational disorder of one CF_3 group in **10** was resolved and refined with 90/10% occupation applying geometric and ADP restraints. In addition, similarity restraints were applied to refine equivalent geometric parameters of both molecules within the asymmetric unit (**10**). Further details of the crystallographic data are contained in the Supporting Information.

NMR spectra were recorded on a Bruker DMX-500 spectrometer operating at 500.13 MHz for protons, and are reported in δ (ppm) relative to internal tetramethylsilane (TMS). The NOESY spectrum was run in toluene-d_8 solution at 250 K with a standard pulse sequence for a phase-sensitive spectrum, using a NOE evolution time of 300 ms. Elemental analyses were performed by Mikroanalytisches Laboratorium Beller, Göttingen, Germany.

Bis(*N*-(dimethylamino)trifluoroacetimidato-*N*,*O*)fluoro(phenyl)-silicon(IV) (6).[11] A solution of 1.368 g (0.006 mol) of $Me_3SiOC(CF_3)$═$NNMe_2$[16] (**16**) and 0.49 g (0.003 mol) of $PhSiF_3$ in 2 mL of dry toluene was allowed to react under a dry argon atmosphere. The mixture was evacuated followed by refrigeration at −20 °C for a week. Crystallization was effected by the addition of petroleum ether (40−60 °C) until the solution turned turbid, followed by 24 h at −20 °C. **6**

(22) Kottke, T.; Stalke, D. *J. Appl. Crystallogr.* **1993**, *26*, 615.
(23) Sheldrick, G. M. *Acta Crystallogr.* **1990**, *A46*, 467.
(24) Sheldrick, G. M. *Program for crystal structure refinement*, University of Göttingen, Germany, 1996.

crystallized out in essentially quantitative yield, the solution was decanted off under reduced pressure, and the crystals were dried under low pressure, mp 89−90 °C. An analytical sample and a single crystal suitable for crystallography were taken directly from this product. ^{1}H NMR (CD_2Cl_2, 300 K): δ 2.23 (br s, 3H, N*Me*), 2.68 (br s, 6H, N*Me*), 3.10 (br s, 3H, N*Me*), 7.30−8.00 (m, 5H, Ph). ^{13}C NMR (CD_2Cl_2, 300 K): δ 48.8 (br, N*Me*), 49.8 (br, N*Me*), 52.6 (br, N*Me*), 117.8 (q, CF_3, ^1J(C−F) = 275 Hz), 128−145 (Ph), 157.46 (q, *C*═N, ^2J(C−F) = 38 Hz). ^{29}Si NMR (CD_2Cl_2, 300 K): δ −146.2 (d, ^1J(Si−F) = 280 Hz). Anal. Calcd for $C_{14}H_{17}F_7N_4O_2Si$: C, 38.71; H, 3.92; N, 12.90. Found: C, 38.69; H, 4.02; N, 12.84.

Bis(*N*-(dimethylamino)trifluoroacetimidato-*N,O*)difluorosilicon-(IV) (7).[11] SiF_4, generated by heating of $BaSiF_6$,[25] was passed through a solution of 2 mL of dry toluene and 1.14 g (0.005 mol) of **16** under an argon atmosphere, until a white precipitate had separated. The mixture was evacuated followed by refrigeration at −20 °C. Crystallization was complete after a few days. The solution was decanted, and the crystals were dried in vacuo. An analytical sample and a single crystal were taken without further treatment. ^{1}H NMR ($CDCl_3$, 300 K): δ 2.88 (t, ^4J(F−H) = 1.57 Hz, 6H, NCH_3), 2.95 (t, ^4J(F−H) = 0.71 Hz, 6H, NCH_3). ^{13}C NMR ($CDCl_3$, 300 K): δ 50.04 (t, ^3J(F−C) = 1.3 Hz, N*C*H$_3$), 50.25 (t, ^3J(F−C) = 5.4 Hz, N*C*H$_3$), 116.8 (q, ^1J(F−C) = 276.7 Hz, *C*F$_3$), 157.7 (qt, ^2J(F−C) = 38.6 Hz, ^4J(F−C) = 1.1 Hz, *C*═N). ^{29}Si NMR (CD_2Cl_2, 300 K): δ −159.6 (t, ^1J(Si−F) = 205.7 Hz). Anal. Calcd for $C_8H_{12}F_8N_4O_2Si$: C, 25.54; H, 3.21; N, 14.89. Found: C, 25.52; H, 3.11; N, 14.81.

Bis(*N*-(dimethylamino)trifluoroacetimidato-*N,O*)chloro(phenyl)-silicon(IV) (10). The synthesis was described previously.[16] **10** was crystallized for X-ray crystallography from a toluene solution at −18 °C (mp 129−131 °C). Anal. Calcd for $C_{14}H_{17}ClF_6N_4O_2Si$: C, 37.30; H, 3.80; N, 12.43. Found: C, 36.56; H, 3.91; N, 12.55.

Bis(*N*-(dimethylamino)trifluoroacetimidato-*N,O*)dichlorosilicon-(IV) (11). The synthesis was described previously.[16] **11** was crystallized for X-ray crystallography from a toluene solution at −18 °C. Anal. Calcd for $C_8H_{12}Cl_2F_6N_4O_2Si$: C, 23.48; H, 2.96; N, 13.69. Found: C, 23.68; H, 3.02; N, 13.70.

Bis(*N*-(dimethylamino)-(*R*)-2-phenylpropionimidato-*N,O*)chloro-(phenyl)silicon(IV) (14). (a) (R)-2-Phenyl-2′,2′-dimethylpropiono-hydrazide (1,1-Dimethyl-2-((*R*)-2-phenylpropionyl)hydrazine). The hydrazide was prepared from 0.043 mol (6.42 g) of (*R*)-(−)-2-phenylpropionic acid (Aldrich) by refluxing with 0.086 mol (6.2 mL) of thionyl chloride for 1.5 h, followed by removal of excess $SOCl_2$ under reduced pressure and distillation of the acid chloride, collecting 7.0 g (97%) at 106−107 °C (23 Torr). The chloride was dissolved in 10 mL of CCl_4 and added dropwise with stirring to an ice cold solution of 0.063 mol (3.8 g) of 1,1-dimethylhydrazine and 0.084 mol (8.5 g) of triethylamine in 80 mL of CCl_4, keeping the temperature below 4 °C. The mixture was allowed to warm to room temperature with stirring for another 3 h. The precipitate was filtered off and the product was crystallized out by addition of petroleum ether (40−60 °C). Mp: 100−101 °C (mp of racemic compound 80−81 °C). Yield: 7.6 g (94%). ^{1}H NMR ($CDCl_3$): δ 1.43, 1.48 (2d, ^3J = 7 Hz, 3H, (*E,Z*) CCH_3), 2.50 (s, 6H, NCH_3), 3.47, 4.34 (2q, ^3J = 7 Hz, 1H, (*E,Z*) C*H*), 7.2−7.4 (m, 5H, Ph). Anal. Calcd for $C_{11}H_{16}N_2O$: C, 68.72; H, 8.39; N, 14.57. Found: C, 68.13; H, 8.27; N, 14.62.

(b) *O*-Trimethylsilylated 1,1-Dimethyl-2-((*R*)-2-phenylpropionyl)-hydrazine. The hydrazide from (a) (0.0396 mol, 7.6 g) was dissolved in 100 mL of toluene with 0.079 mol (11 mL) of triethylamine under dry argon. To this solution was added dropwise and with stirring a trimethylchlorosilane (0.0475 mol, 6 mL) solution in 10 mL of toluene at ambient temperature. The reaction was refluxed for 20 h, after which it was cooled to room temperature and filtered under argon. The filtrate was distilled to yield 8.5 g (0.032 mol, 81% yield), collected between 66 and 68 °C (0.4 Torr). ^{1}H NMR ($CDCl_3$): δ 0.03, 0.22 (2s, 9H, (*E,Z*) SiCH_3), 1.39, 1.45 (2d, ^3J = 7.2 Hz, 3H, (*E,Z*) CCH_3), 2.31, 2.33 (2s, 6H, (*E,Z*) NCH_3), 3.63, 4.77 (2q, ^3J = 7.2 Hz, 1H, C*H*), 7.21−7.34 (m, 5H, Ph). ^{13}C NMR: δ 0.2, 0.5 (2s, (*E,Z*) Si*C*H$_3$), 17.4, 18.2 (2s, (*E,Z*) C*C*H$_3$), 37.6, 44.5 (2s, (*E,Z*) *C*H), 46.6, 48.5 (2s, (*E,Z*) N*C*H$_3$), 126−128 (m, Ph), 141.5, 142.4 (2s, (*E,Z*) *ipso*-Ph), 162.2, 169.1 (2s, (*E,Z*) *C*═N). ^{29}Si NMR ($CDCl_3$): δ 17.7, 20.4 ((*E,Z*) isomers).

(c) 14. The complex was prepared directly in an NMR tube, from 0.25 g of product (b) and 0.1 g of $PhSiCl_3$, in the appropriate deuterated solvent. Attempts to prepare **14** (and its racemic mixture) on a larger scale did not result in crystallization or isolation of pure complex. However, **14** is identified by analogy of its NMR spectrum with those of other complexes in the series. ^{1}H NMR ($CDCl_3$): δ 1.44, 1.51 (2d, ^3J = 7 Hz, 6H, (*RRR*) and (*RSR*) CCH_3), 2.34, 2.36, 2.75, 2.77 (4s, 12H, (*RRR*) and (*RSR*) NCH_3), 3.47, 3.70 (2 br s, 2H, (*RRR*) and (*RSR*) C*H*), 7.0−7.8 (m, 15H, Ph). ^{13}C NMR ($CDCl_3$): δ 17.2 (s, C*C*H$_3$), 41.85, 41.97 (2s, (*RRR*) and (*RSR*) *C*H), 51.14, 51.29, 51.36 (3s, N*C*H$_3$), 127−143 (m, Ph), 169.79, 169.93 (2s, *C*═N). ^{29}Si NMR ($CDCl_3$): δ 130.5, 131.6 ((*RRR*) and (*RSR*) isomers).

Acknowledgment. We thank the Israeli Ministry of Sciences and Arts and the Israel Science Foundation (administered by the Israel Academy of Sciences and Humanities) for financial support.

Supporting Information Available: Tables of crystal data, fractional coordinates and *U* values, bond distances and angles, anisotropic displacement parameters, and hydrogen atom coordinates and completely labeled figures of structures **10** and **11** (21 pages, print/PDF). See any current masthead page for ordering information and Web access instructions.

JA9730021

(25) MacDiarmid, A. G. In *Preparative Inorganic Reactoins*; Jolly, W. L., Ed.; Interscience: New York, 1964; Vol. 1, p 185.